

A first-principles model of copper–boron interactions in Si: implications for the light-induced degradation of solar Si

E Wright¹, J Coutinho¹, S Öberg² and V J B Torres¹

¹ Department of Physics and I3N, University of Aveiro, Campus Santiago, 3810-193 Aveiro, Portugal

² Department of Engineering Sciences and Mathematics, Luleå University of Technology, SE-97187 Luleå, Sweden

E-mail: wrighteap@ua.pt

Received 5 August 2016, revised 9 November 2016

Accepted for publication 14 November 2016

Published 19 December 2016



Abstract

The recent discovery that Cu contamination of Si combined with light exposure has a significant detrimental impact on carrier life-time has drawn much concern within the solar-Si community. The effect, known as the copper-related light-induced degradation (Cu-LID) of Si solar cells, has been connected to the release of Cu interstitials within the bulk (2016 *Sol. Energy Mater. Sol. Cells* **147** 115–26). In this paper, we describe a comprehensive analysis of the formation/dissociation process of the CuB pair in Si by means of first-principles modelling, as well as the interaction of CuB defects with photo-excited minority carriers. We confirm that the long-range interaction between the Cu_i^+ cation and the B_s^- anion has a Coulomb-like behaviour, in line with the trapping-limited diffusivity of Cu observed by transient ion drift measurements. On the other hand, the short-range interaction between the d-electrons of Cu and the excess of negative charge on B_s^- produces a repulsive effect, thereby decreasing the binding energy of the pair when compared to the ideal point-charge Coulomb model. We also find that metastable CuB pairs produce acceptor states just below the conduction band minimum, which arise from the Cu level emptied by the B acceptor. Based on these results, we argue that photo-generated minority carriers trapped by the metastable pairs can switch off the Coulomb interaction that holds the pairs together, enhancing the release of Cu interstitials, and acting as a catalyst for Cu-LID.

Keywords: silicon, light-induced degradation (LID), copper, boron

(Some figures may appear in colour only in the online journal)

1. Introduction

Owing to the extremely high diffusivity of copper in Si, the large majority of Cu contaminants in the bulk precipitate into silicides, decorate existing extended defects, such as dislocations or grain boundaries, or out-diffuse towards the surface [1]. Additionally, a small but unavoidable fraction of Cu atoms linger within the bulk, and these are capable of forming various electrically-active defects, like interstitial Cu (Cu_i), substitutional Cu (Cu_s) [2], combinations of both these defects, [3, 4], as well as complexes containing copper and other species like oxygen, transition metals and dopants [5]. Interest in

the physics and chemistry of Copper was recently renewed, in the context of the light-induced degradation (Cu-LID) of solar silicon [6], an effect whereby above-bandgap illumination or forward biasing results in the reduction of minority carrier life-times in solar cells [7, 8], but which can be prevented through the forced out-diffusion of positively-charged Cu (Cu_i^+) impurities [9]. Notably, the underlying recombination centre remains unknown [10].

As a point defect, Cu occurs primarily as Cu_i^+ , except in $\text{n}^+\text{-Si}$ or in the presence of vacancies, where Cu is found as Cu_s^- [11]. Precipitation occurs mostly in the form of amphoteric Cu silicides (Cu_3Si), and is favoured in n-type material

over p-type material [12]. In fact, precipitation in B-doped Si at room temperature occurs only for interstitial Cu concentrations $[\text{Cu}_i] \gtrsim [\text{B}_s] + 10^{16} \text{ cm}^{-3}$, where $[\text{B}_s]$ is the concentration of substitutional B [13]. Below this threshold, the favourable reaction paths for Cu are out-diffusion or pairing with B atoms driven by the Coulomb attraction between Cu_i^+ and B_s^- ionic charges [14, 15].

Although CuB pairs are thought to be electrically inactive, their association/dissociation dynamics limit the Cu-LID rate, at the very least—the effect slows down with increasing $[\text{B}_s]$, speeds up with temperature, and both the concentration of the underlying LID-defect and the activation energy for the rate of degradation ($E_{\text{a,LID}}$) increase with $[\text{B}]$, as well as with $[\text{Ga}]$ [6].

The current understanding of the association/dissociation dynamics of CuA pairs (where A stands for a group-III dopant species) is based on a diffusion-limited trapping model of Cu_i^+ . In the absence of A_s^- dopants, the average thermal energy of copper ions (β) causes them to diffuse randomly through the tetrahedral interstitial sites of the Si lattice [16, 17]. In the presence of A_s^- dopants, and for Cu_i^+ - A_s^- separations for which the attractive potential matches β , Cu_i^+ is assumed trapped by A_s^- , forming a CuA pair with zero net charge. This model was employed to explain the observed reduction in the diffusivity of Cu_i^+ as a function of the acceptor concentration (N_{a}), with respect to the intrinsic value (D_{int}). Accordingly, transient ion drift (TID) measurements in p-Si have shown that the effective diffusivity of Cu_i^+ (D_{eff}) decreases for increasing acceptor concentrations based on the following semi-empirical expression [14, 17–19],

$$D_{\text{eff}}(N_{\text{a}}, \beta) = \frac{D_{\text{int}}}{1 + (C/\beta) N_{\text{a}} D_{\text{int}} \tau_{\text{diss}}}, \quad (1)$$

where $\beta \equiv k_{\text{B}}T$ in eV (k_{B} is the Boltzmann constant and T the temperature) and $C \equiv e/(\epsilon_{\text{r}}\epsilon_0) \times 10^2$ in $\text{eV} \cdot \text{cm}$ (e , ϵ_{r} and ϵ_0 are the elementary electron charge, the relative permittivity of the bulk and the vacuum permittivity, respectively—in SI units), and N_{a} and D_{int} are in cm^{-3} and $\text{cm}^2 \text{ s}^{-1}$, respectively. The dissociation rate (τ_{diss}) for the CuA pair and D_{int} can be obtained experimentally, and fittings to the corresponding temperature-dependent data yield the dissociation energy of the CuA pair (E_{d}) and the migration barrier (E_{m}) of Cu_i^+ respectively [14, 17].

The derivation of equation (1) assumes that the covalent interaction between Cu_i^+ and A_s^- is negligible, and the binding energy (E_{b}) of CuA pairs is independent of the species A. Assuming that in the ground state of the pair (i) the Cu and A ions are separated by a distance equivalent to that of the crystalline Si–Si bond length, i.e. that they are located at nearest neighbouring interstitial and substitutional sites, respectively, and that (ii) their interaction is well described by a two-point-charge model mediated by the static dielectric constant of Si³, one arrives at a binding energy $E_{\text{b}} = 0.52 \text{ eV}$ and a value of

$E_{\text{d}} \simeq E_{\text{m}} + E_{\text{b}} = 0.70 \text{ eV}$, where $E_{\text{m}} = 0.18 \pm 0.01 \text{ eV}$ has been determined experimentally [17]. While this produces good agreement with the experimental values of E_{d} for CuAl, CuGa, and CuIn pairs, $0.70 \pm 0.02 \text{ eV}$, $0.71 \pm 0.02 \text{ eV}$ and $0.69 \pm 0.02 \text{ eV}$ respectively, the same is not true for CuB pairs, where $E_{\text{d}} = 0.61 \pm 0.02 \text{ eV}$ [1, 14]. An attempt to explain this effect has been reported by Estreicher [15] employing the Hartree–Fock method and H-terminated Si clusters. Accordingly, a Cu_i^+ ion bound either to a substitutional B, Al or Ga ion was moved to the next T-site along the $\langle 111 \rangle$ direction (through the H hexagonal ring), resulting in metastable pairs with energies 0.45 eV, 0.64 eV and 0.68 eV above that of their respective ground states. These figures and the respective chemical trend were in good agreement with experimental observations, but as carefully noted by the author [15], they are not entirely consistent with the plain-Coulomb model underlying equation (1). In particular, the results suggest that the dissociation process is dominated by a short-range interaction, as the activation energy for the very first step which breaks up the CuA pair exceeds the long-range electrostatic dissociation energy.

The aim of this paper is two-fold: (i) to provide an in-depth analysis of the dissociation process of the CuB pair in Si using first-principles methods, and (ii) to inspect the interaction of CuB defects with photo-excited carriers in the context of Cu-LID. Starting with the ground-state structure of the CuB pair, the energy barriers for the first dissociating steps are calculated. This allows us to inspect for any hypothetical dissociation barrier greater than the sum of the long-range Coulomb binding energy and the migration energy of Cu_i^+ . Next, the stability of the intermediate metastable states of the CuB pair is analysed as a function of the distance between Cu_i^+ and B_s^- , their electronic activity and interaction with minority carriers (electrons) is calculated and discussed. Finally, the energy to attain a fully dissociated pair is estimated by means of independent supercells containing neutral Cu_i^0 and B_s^0 and subtracting the charge-transfer energy due to electron donation from Cu to B.

2. Method

All calculations were computed using the VASP package [20–23], employing the projector-augment wave (PAW) [24, 25] method and a planewave basis set, within the generalised gradient approximation to the exchange-correlation potential among electrons, as proposed by Perdew, Burke and Ernzerhof [26]. The PAW potentials used for Cu, B and Si included the valence states given by the corresponding electronic configurations: $3p^6 3d^{10} 4s^1$, $2s^2 2p^1$ and $3s^2 3p^2$. Following convergence tests, the maximum planewave kinetic energy was set to $E_{\text{cut}} = 370 \text{ eV}$.

Cu, B and CuB point defects were inserted into 216-atom Si supercells, with a cubic shape and an optimised lattice constant $a = 5.4687 \text{ \AA}$. All defect structures were optimised using either a conjugate-gradient method or a quasi-Newton algorithm, until the forces acting on the atoms were converged within $1 \times 10^{-3} \text{ eV \AA}^{-1}$. The self-consistent electronic and magnetic relaxations were computed with an accuracy of $1 \times 10^{-5} \text{ eV}$,

³ Although the aim of this paper is not to discuss the type of bond between Cu and the acceptor, the short distance between the Cu and A atoms in the ground state implies that a description based on macroscopic electrostatics is highly debatable.

and the band structures were sampled at \mathbf{k} -points defined by $2 \times 2 \times 2$ Monkhorst–Pack grids (avoiding the Γ -point) [27].

The marker method was employed to assess the electronic activity of CuB complexes [28]. To this end, $\text{Cu}_i(0/+) = E_C - 0.15 \text{ eV}$ [29] and $\text{B}_s(-/0) = E_V + 0.045 \text{ eV}$ [30] were used as marker levels, corresponding to the calculated ionisation potential and affinity energies $I\{\text{Cu}_i(0/+)\} = 6.247 \text{ eV}$ and $A\{\text{B}_s(-/0)\} = 5.582 \text{ eV}$, respectively. The spurious long-range interactions arising from the periodic arrangement of localised charged defects (immersed in a compensating background *jellium*) was accounted for by an image-charge correction $E_{\text{chg}}[D^q]$ as proposed in [31, 32]. This term depends on the shape of the ionised density of a particular defect D in charge state q , and was added to the total energies of defective supercells. For the defects under scrutiny, and for first ionisation and affinity energies, image-charge corrections were all close to $E_{\text{chg}} \sim 80 \text{ meV}$. Since the marker method relies on differences between the values of I (or A) calculated for the marker defect and the inspected defect, these correction terms mostly cancel out, and the net contributions are on the order of a few meV.

The defects reported in this work comprise copper–boron pairs with different separations. Each pair is expected to form an electric dipole, not only within the hosting cubic cell, but also in all periodic cell replicas. This introduces a spurious long-range dipole-image interaction term in the total energy. This term is ill-defined with respect to the origin of the coordinate system and it is not trivial to account for [33]. To estimate how large this dipole-image error can be, we calculated the total energy of two CuB pairs (in their ground state structure with C_{3v} symmetry) in the same cell, which was chosen to have a hexagonal shape (with 382 atoms and lattice parameters $a = b = 15.468 \text{ \AA}$, $c = 37.888 \text{ \AA}$). Both defects were collinearly aligned along the $[111]$ crystallographic axis and separated by a distance of $c/2$, with parallel dipole moments and antiparallel dipole moments (as depicted in figure 1(b)), yielding total energies denoted $E_{\uparrow\uparrow}$ and $E_{\uparrow\downarrow}$, respectively. Since the latter energy corresponds to a system with zero net dipole moment, we arrive at the dipole-image correction,

$$E_{\text{dip}} = (E_{\uparrow\downarrow} - E_{\uparrow\uparrow})/2 = 0.013 \text{ eV}, \quad (2)$$

per Cu–B pair. Such a small figure, allows us to safely neglect any dipole-image corrections to the calculations presented below, even considering error bars of the order of 0.1–0.2 eV.

The potential energy surface (PES) governing the motion of a Cu_i^+ ion close to B_s^- was investigated using the nudged elastic band (NEB) method [34]. Using this method, we were able to calculate the energy barriers and the minimum energy paths (MEP) connecting neighbouring tetrahedral interstitial sites using 7 intermediate structures. For the NEB calculations, the forces acting on the atoms were converged within $1 \times 10^{-2} \text{ eV \AA}^{-1}$.

3. Results

The present description of the dissociation process of CuB pairs is based on the first-principles calculation of four parameters, namely (1) the activation energy (E_a) required to break

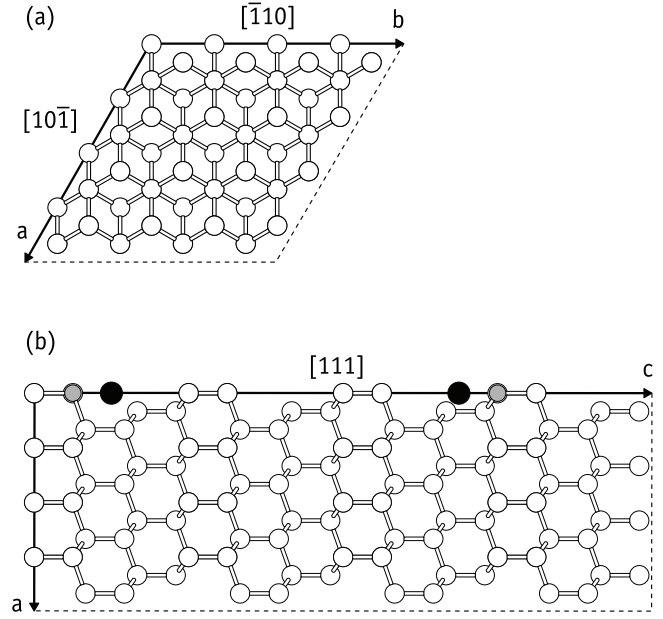


Figure 1. Projections of the hexagonal cell ($a = b = 15.468 \text{ \AA}$, $c = 37.888 \text{ \AA}$) used in the calculation of the dipole-image interaction energy, along (a) the $[111]$ and (b) $[\bar{1}10]$ crystallographic cubic directions, depicting two CuB defects with antiparallel dipole moments. Si atoms are represented in white, B in grey and Cu in black.

up a stable CuB pair and transform it into a metastable configuration, (2) the dissociation energy (E_d) required to separate Cu_i^+ and B_s^- ions beyond their long-range Coulomb interaction distance, (3) the migration energy (E_m) of Cu_i^+ in pristine crystalline Si, and (4) the binding energy (E_b) holding a CuB pair together, with respect to uncorrelated Cu_i^+ and B_s^- defects. These parameters characterise the process, in the manner depicted in figure 2(a).

We start by reporting on the energetics of supercells containing the CuB ground state and its first seven metastable configurations. The energy of the pairs with respect to infinitely separated Cu_i^+ and B_s^- defects are reported as blue circles in figure 2(b). The calculation of the energy reference (for the infinitely separated ions) is discussed in detail further below. The left vertical axis in figure 2(b) represents the reversed binding energy of a CuB complex for a Cu atom sitting at the n th neighbouring site relative to the B atom, as indicated by the upper horizontal axis. The lower horizontal axis represents the respective separation between Cu and B nuclei. The first four configurations corresponding to the shortest Cu–B distances are depicted in figure 3. The energies of sites 2–8 are 0.21, 0.19, 0.18, 0.19, 0.23, 0.25 and 0.26 eV above that of the ground state (site 1), respectively. These figures reveal a prominent stabilisation of site 1 when compared to more distant sites. Further, the interaction potential for sites 2–5 is approximately constant. These results clearly indicate that the Cu–B interaction involves a short-range effect which is not accounted for by a Coulomb term alone.

In order to explore the PES of a moving Cu ion in the neighbourhood of a B acceptor, we calculated the energy barriers $E_a^{1,2}$ and $E_a^{1,4}$ that account for Cu jumps from site 1

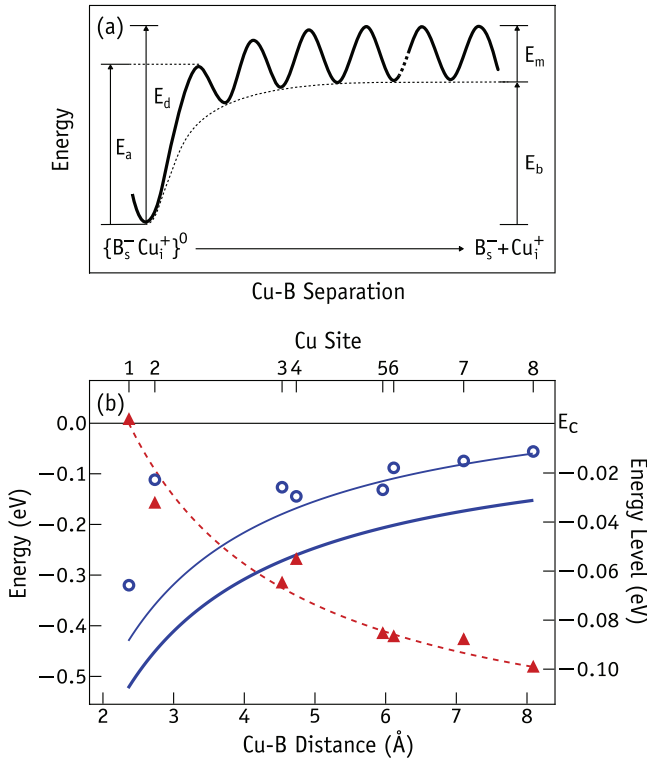


Figure 2. (a) Schematic representation of the potential energy for the $\{Cu_i^+ B_s^-\}^0 \rightarrow Cu_i^+ + B_s^-$ dissociation mechanism, as a function of the distance between Cu_i^+ and B_s^- ions (see the beginning of this section for a description of the energy parameters). (b) Relative energies of CuB pairs (blue circles) and respective acceptor levels (red triangles). Defect energies are given with respect to infinitely separated Cu_i^+ and B_s^- ions (left-vertical axis). Electrical levels are represented with respect to the bottom of the conduction band (E_C) as indicated by the right-vertical axis. The lower-horizontal axis indicates the distance between the ions, while the upper axis refers to the n th neighbouring site of Cu with respect to B ($n = 1, \dots, 8$). The thick full line represents a screened Coulomb potential energy V_C of two point charges of opposite sign, while the thin full line shows $V_C + 0.1$ eV (see text). The dashed line is a mere guideline.

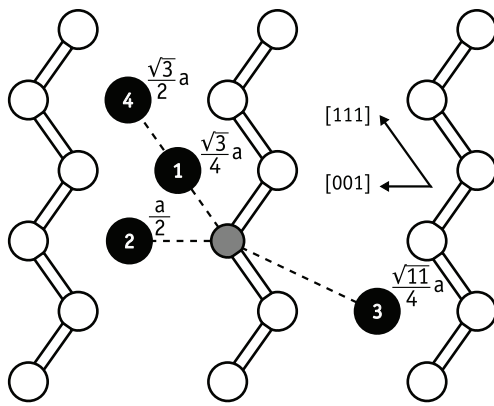


Figure 3. Slice of a Si crystal along the $(1 \bar{1} 0)$ plane containing a B_s dopant (grey atom close to the centre) and its first four tetrahedral interstitial neighbouring sites, which can be occupied by a Cu atom (numbered 1 to 4). Site distances to the B atom are also quoted in units of the Si lattice constant (a).

Table 1. A comparison of the values calculated for the relevant energy barriers in the Cu-B association/dissociation process, compared to other calculations and experimental values in the literature, in eV.

	Calculated	Previous calculations	Experimental
E_m	0.11	0.18 [35], 0.24 [15]	0.18 [17]
E_b	0.32	—	0.43 ^a
E_d	0.43	> 0.69	0.61 [14]
$E_a^{1,2}$	0.32	—	—
$E_a^{1,4}$	0.35	0.45 [15]	—

^aThis figure was calculated by assuming that $E_b = E_d - E_m$.

(ground state) to sites 2 and 4, respectively. Site 3 is too distant (along the configurational space) from site 1, and is more likely to be reached through site 2. For these calculations, the supercells were kept neutral, and as we will see below, in the absence of above-bandgap illumination the Cu atom hops around B_s^- as a positively charged ion. The results are reported in table 1. Although $E_a^{1,4}$ is 0.03 eV higher than $E_a^{1,2}$, the difference is within the precision of the methodology, suggesting that the pair is able to break up either along sites 1-4... or 1-2-3... Regardless of the path, the very first activation barrier to the break-up of a CuB pair is just over $E_a \sim 0.3$ eV. This is about 3 times the calculated migration barrier of isolated Cu_i^+ , which was estimated as $E_m = 0.11$ eV using the NEB method between neighbouring interstitial sites in a positively charged supercell without boron (only 70 meV lower than the experimental value of 0.18 eV for Cu migration in intrinsic Si without traps). Finally, considering the relative energies of sites 2, 3 and 4, we also conclude that the barrier for the reverse process, i.e. for the capture of Cu_i^+ by B_s^- , is about 0.1 eV and very close to E_m , suggesting that the short-range interaction between Cu and B affects the association/dissociation kinetics at the nearest sites only (perhaps 1–3). Beyond that, the Coulomb interaction starts to dominate.

Next, the binding energy of the pair (E_b) was calculated, and the dissociation energy ($E_d = E_b + E_m$) was compared to $E_a^{1,2}$ and $E_a^{1,4}$. This allowed us to investigate whether the macroscopic association/dissociation kinetics is dominated by a short-range breaking/capture barrier, or by the long-range shape of the Coulomb potential (added to the barrier for migration of Cu_i^+ through the lattice). The value of E_b was obtained by considering the energy gained by taking uncorrelated Cu_i^+ and B_s^- , and combining them into a neutral $\{Cu_i^+ B_s^-\}^0$ pair. While the calculation of the final state is straightforward, for the initial state the method must account for the compensation of Cu by the B dopant. The energy required to infinitely separate Cu_i^+ from B_s^- was therefore calculated as follows

$$E(Cu_i^+ + B_s^-) = E(Cu_i^0) + E(B_s^0) - \Delta E_{CT}, \quad (3)$$

where $E(Cu_i^0)$ and $E(B_s^0)$ are the energies of neutral Cu_i and B_s defects calculated in separate supercells. The quantity ΔE_{CT} accounts for the charge transfer energy that is released after demotion of an electron from the Cu gap state to an

infinitely distant B acceptor. We obtain this quantity from $\Delta E_{CT} = A\{B_s(-/0)\} - I\{Cu_i(0/+)\} = 0.66$ eV, which effectively is the energy difference between the calculated $Cu_i(0/+)$ and $B_s(-/0)$ levels. We note that the underestimated band gap of Si (due to the semi-local treatment of the exchange-correlation energy), leads to analogous errors in the calculation of the ΔE_{CT} term and $E(Cu_i^0) + E(B_s^0)$ terms in equation (3), which are expected to cancel out. After fixing any stoichiometric mismatch in the number of Si atoms in the calculation, the aforementioned considerations result in $E_b = 0.32$ eV, which underestimates the experimental value by 0.1 eV only. We note that if the charge transfer term had not been considered, the (first-principles) binding energy for the $Cu_i^0 + B_s^0 \rightarrow \{Cu_i^+ B_s^-\}^0$ reaction would be 1.22 eV. Adding this value to the migration barrier of copper yields a dissociation barrier of 1.4 eV, in obvious disagreement with the observations. Nevertheless, our estimate for E_d is 0.43–0.50 eV, depending on whether we add the calculated or the experimental value of E_m to the binding energy, and this is well in line with a defect that is marginally stable at room temperature. Finally, we note that E_d is larger than both $E_a^{1,2}$ and $E_a^{1,4}$, indicating that the dissociation of the pair involves the migration of Cu_i^+ under the action of an attractive long-range Coulomb potential, which it must eventually escape from.

Figure 2(b) shows a thick solid line that represents the interatomic potential energy of two unitary point charges, $V_C = -\kappa_e/r$, screened by the dielectric constant of bulk Si ($\epsilon_r = 11.68$), where κ_e is the Coulomb constant in eV Å. In the same figure we represent $V(r) + 0.1$ eV by a thin solid line. This allows us to directly compare the first-principles data to the Coulomb potential, after adding 0.1 eV to the latter, the energy corresponding to the deviation between the calculated and the experimental values of the binding energy. From the figure, we conclude that, while a repulsive *central-cell* correction of about 0.1–0.2 eV has to be considered in order to obtain agreement between the Coulomb model and the first-principles data for sites 1 and 2, agreement is rather good for remote sites. When compared to the Coulomb potential, the additional energy for sites 1 and 2 could be ascribed to a finite size effect like the increase in the overlap of the 3d electrons of Cu to the excess of negative charge close to the B_s^- ion.

The electronic activity of the various CuB pair structures was also investigated. Despite the lack of evidence for carrier trapping or recombination activity due to CuB complexes, the reason behind such inert behaviour is actually uncharted. Further, this inactivity has been asserted for the CuB ground state only, and nothing is known about the metastable configurations. This aspect could be relevant in the context of Cu-LID, particularly in p-type Si, since it could support a direct connection between a hypothetical light-enhanced dissociation of CuB pairs (and therefore the release of Cu) and the observed decrease in minority carrier life-time.

The calculated ionisation energies of CuB pairs are mostly independent of the distance between B_s^- and Cu_i^+ ions, $I\{CuB(0/+)\} = 5.50(5)$ eV (for sites 1–8). This figure should be compared to $A\{B_s(-/0)\} = 5.582$ eV, indicating that

CuB(0/+) transitions are about 80 meV below the boron level, and effectively suggesting that none of the CuB defects have donor levels in the gap. As a word of caution, we note that such small energies are well within the error bar of the method, and an eventual shallow hole trap related to CuB(0/+) could be effectively undetectable as it could lie just below the $B_s(-/0)$ transition. We also point out that the weak dependence of the CuB(0/+) levels on the Cu-B distance stems from the fact that they derive from the shallow boron state (here fully occupied due to an electron donated by Cu). The low amplitude and extensive spatial distribution of the state means that it is unlikely to be sensitive to the relative position of a localised Cu_i^+ ion.

Next we investigated the acceptor activity of CuB pairs. Comparing the affinities of the various CuB defects with the ionisation potential of Cu_i we arrive at CuB(-/0) levels ranging from $E_C - 0.00$ eV (for the ground state) to approximately $E_C - 0.10$ eV (for Cu at site 8). The results are reproduced graphically in figure 2(b) (refer to the right-vertical axis), along with the dashed line that clearly indicates a trend towards the isolated $Cu_i(0/+)$ transition (experimentally measured at $E_C - 0.15$ eV [29]) when the ions become infinitely separated. The calculations support the prevailing ground-state model as an electronically inactive defect. However, they also anticipate that the pairs turn into acceptors as soon as the ion separation becomes larger than the first neighbouring distance. All calculated CuB(-/0) transitions edge the conduction band minimum and derive from the $Cu_i(0/+)$ transition, which is shifted up in the energy scale due to Coulomb repulsion by the B_s^- anion. An analogous argument was used to explain the location of the FeB(-/0) level in Si as arising from a $Fe_i(0/+)$ transition displaced by B_s^- [36].

Since CuB pairs are marginally stable at room temperature, our results suggest that in B-doped Si, photo-excited electrons could be trapped at the Cu atom of a metastable CuB complex, effectively *turning off* the Coulomb binding potential between the pair. If this $B_s^- Cu_i^0$ state survives for a sufficiently long time before the electron is emitted back into the conduction band, it is likely that a light-induced dissociation enhancement of CuB pairs will take place, explaining the doping/illumination dependence of Cu-LID on the basis of the change in the dynamics of the binding/dissociation of mobile copper to/from acceptors during a diffusion-limited process.

The nature of the defect behind Cu-LID remains unknown. Recently, Lindroos and Savin [10] hypothesised a possible involvement of either substitutional copper or copper precipitates in the recombination-active centre. It is also known that illumination leads to a decrease of interstitial copper in silicon [37]. Based on these premisses, we investigated the light-induced transformation of Cu_i into Cu_s through the $Cu_i^+ B_s^- \xrightarrow{h\nu} Cu_s^- + B_i^+$ reaction, eventually made possible with the help of about 1 eV resulting from the recombination between a photo-excited electron trapped at a metastable CuB pair, and a free-hole. To this end we compared the relative stability of $Cu_i B_s$ and $Cu_s B_i$ defects in neutral cells. Note that the first acceptor level of Cu_s (at $E_V + 0.09$ eV [38]) lies below the donor level of B_i (at $E_C - 0.13$ eV [39]), implying that neutral

Cu_sB_i is actually a $\text{Cu}_s^-\text{B}_i^+$ ionic complex, where the boron atom is located close to the tetrahedral interstitial site, toward the Cu site. We found that Cu_iB_s is more stable than Cu_sB_i by about 2.0 eV. It is thus reasonable to assume that the exchange transformation $\text{Cu}_i\text{B}_s \rightarrow \text{Cu}_s\text{B}_i$ should have a barrier in excess of the 2 eV energy difference. Although we can not exclude the involvement of substitutional copper in the Cu-LID defect, such a large barrier suggests that at room-temperature Cu_s cannot be formed directly from the interaction of Cu_i with B_s , even with the assistance of above-bandgap illumination.

4. Conclusions

In conclusion, a first-principles model of the association/dissociation mechanism of CuB pairs in Si has been presented. This model is based on calculations of (1) the activation energy (E_a) required to transform a stable CuB pair into a metastable configuration, (2) the dissociation energy (E_d) required to separate Cu and B ions beyond their long-range Coulomb interaction distance, (3) the migration energy (E_m) of Cu_i^+ in pristine crystalline Si, and (4) the binding energy (E_b) holding the CuB pair together. In calculating E_a , it was determined that the energy barrier that a Cu atom in the CuB ground state complex has to overcome in order to reach the next interstitial site is approximately 0.3 eV smaller than the experimental value of $E_d \simeq E_m + E_b$, and approximately 0.1 eV smaller than the value of E_d calculated in the present work. This suggests that dissociation is limited by the migration of Cu_i^+ under the action of an attractive long-range Coulomb potential (and not by a short-range *bond-breaking* barrier), and also supports the diffusion-limited trapping model used to determine the experimental value of E_d , for large separations between Cu and B ions.

Further analysis based on the energetics of the stable CuB pair, and of its 7 nearest-neighbouring metastable configurations, corroborates previous suggestions that a short-range effect has an influence on the stability of the ground state. In particular, we found that the energies of the stable CuB pair, and of the first nearest-neighbouring metastable configuration, are respectively 0.1 eV and 0.2 eV larger than expected for a Coulomb interaction alone. This is tentatively assigned to the inability of the point-charge Coulomb model to describe the overlap between the closed shell d-electrons of Cu_i^+ and the excess of negative charge in B_s^- . For Cu-B separations greater than the 4th neighbouring distance, the relative energies of the supercells are in relatively good agreement with a long-range Coulomb potential mediated by the static dielectric constant of Si.

The role of the association/dissociation dynamics of CuB pairs in Cu-LID was investigated through calculations of the electronic activity of all CuB configurations. The calculations suggest that while CuB pairs do not have donor levels in the gap, all nearest-neighbouring metastable configurations do have acceptor levels, ranging from $E_C - 0.03$ eV to $E_C - 0.10$ eV, which become deeper with increasing Cu-B separation, and tend to the $E_C - 0.15$ eV level of isolated Cu_i^+ .

Notably, and given the marginal stability of CuB pairs at room temperature, this electronic activity suggests that under sunlight illumination a *quasi-equilibrium* population of photo-excited electrons may be trapped at Cu atoms in metastable configurations of CuB pairs. Should the metastable configurations last long enough, the trapped carriers effectively shield the Cu ions from the attractive potential of B_s^- until they are emitted back into the conduction band. This explains the dependence of the Cu-LID rate on doping/illumination in B-doped Si on the basis of an increased release and diffusivity of Cu interstitials.

As the exact defect underlying Cu-LID remains unknown, and in an attempt to conciliate the fact that (i) Cu-LID is reversed by forcing Cu out-diffusion [9] and that (ii) illumination leads to a decrease of interstitial copper in Si [37], a possible light-induced transformation of Cu_i into Cu_s through a $\text{Cu}_i^+\text{B}_s^- \xrightarrow{h\nu} \text{Cu}_s^- + \text{B}_i^+$ reaction was also investigated. We found that the process is endothermic, as the difference between the energies of two neutral supercells containing $\text{Cu}_i^+\text{B}_s^-$ and $\text{Cu}_s^-\text{B}_i^+$ defects is 2.0 eV (favouring the former structure). This suggests that at room-temperature Cu_s^- cannot result from an interaction between Cu_i and B_s , even if assisted by about 1 eV resulting from an eventual non-radiative recombination between a photo-excited electron trapped by a metastable CuB pair and a free hole.

Acknowledgments

This work was funded by the Fundação para a Ciência e a Tecnologia (FCT) under projects PTDC/CTM-ENE/1973/2012 and UID/CTM/50025/2013, and funded by FEDER funds through the COMPETE 2020 Program. The authors would like to acknowledge the contribution of the COST Action MP1406. Computer resources were provided by the Swedish National Infrastructure for Computing (SNIC) at PDC.

References

- [1] Istratov A A and Weber E R 2002 Physics of copper in silicon *J. Electrochem. Soc.* **149** G21
- [2] Knack S, Weber J, Lemke H and Riemann H 2002 Copper-hydrogen complexes in silicon *Phys. Rev. B* **65**
- [3] Thewalt M L W *et al* 2007 Can highly enriched ^{28}Si reveal new things about old defects? *Physica B* **401–2** 587–92
- [4] Shirai K, Yamaguchi H, Yanase A and Katayama-Yoshida H 2009 A new structure of Cu complex in Si and its photoluminescence *J. Phys.: Condens. Matter* **21** 064249
- [5] Knack S 2004 Copper-related defects in silicon *Mater. Sci. Semicond. Process.* **7** 125–41
- [6] Lindroos J and Savin H 2014 Formation kinetics of copper-related light-induced degradation in crystalline silicon *J. Appl. Phys.* **116** 234901
- [7] Hashigami H, Itakura Y and Saitoh T 2003 Effect of illumination conditions on czochralski-grown silicon solar cell degradation *J. Appl. Phys.* **93** 4240
- [8] Bothe K, Hezel R and Schmidt J 2003 Recombination-enhanced formation of the metastable boron-oxygen complex in crystalline silicon *Appl. Phys. Lett.* **83** 1125

- [9] Boulfrad Y, Lindroos J, Wagner M, Wolny F, Yli-Koski M and Savin H 2014 Experimental evidence on removing copper and light-induced degradation from silicon by negative charge *Appl. Phys. Lett.* **105** 182108
- [10] Lindroos J and Savin H 2016 Review of light-induced degradation in crystalline silicon solar cells *Sol. Energy Mater. Sol. Cells* **147** 115–26
- [11] Bracht H 2004 Copper related diffusion phenomena in germanium and silicon *Mater. Sci. Semicond. Process.* **7** 113–24
- [12] Istratov A A 1998 Electrical and recombination properties of copper-silicide precipitates in silicon *J. Electrochem. Soc.* **145** 3889
- [13] Flink C, Feick H, McHugo S A, Seifert W, Hieslmair H, Heiser T, Istratov A A and Weber E R 2000 Out-diffusion and precipitation of copper in silicon: an electrostatic model *Phys. Rev. Lett.* **85** 4900–3
- [14] Prescha T and Weber J 1992 Interaction of a copper-induced defect with shallow acceptors and deep centers in silicon *Mater. Sci. Forum* **83–7** 167–72
- [15] Estreicher S K 1999 Rich chemistry of copper in crystalline silicon *Phys. Rev. B* **60** 5375–82
- [16] Weber E R 1983 Transition metals in silicon *Appl. Phys. A* **30** 1–22
- [17] Istratov A A, Flink C, Hieslmair H, Weber E R and Heiser T 1998 Intrinsic diffusion coefficient of interstitial copper in silicon *Phys. Rev. Lett.* **81** 1243–6
- [18] Mesli A and Heiser T 1996 Interstitial defect reactions in silicon: the case of copper *Defect Diffus. Forum* **131–2** 89
- [19] Heiser T and Weber E R 1998 Transient ion-drift-induced capacitance signals in semiconductors *Phys. Rev. B* **58** 3893–903
- [20] Kresse G and Hafner J 1993 *Ab initio* molecular dynamics for liquid metals *Phys. Rev. B* **47** 558–61
- [21] Kresse G and Hafner J 1994 *Ab initio* molecular-dynamics simulation of the liquid-metal–amorphous-semiconductor transition in germanium *Phys. Rev. B* **49** 14251–69
- [22] Kresse G and Furthmüller J 1996 Efficiency of *ab initio* total energy calculations for metals and semiconductors using a plane-wave basis set *Comput. Mater. Sci.* **6** 15–50
- [23] Kresse G and Furthmüller J 1996 Efficient iterative schemes for *ab initio* total-energy calculations using a plane-wave basis set *Phys. Rev. B* **54** 11169–86
- [24] Blöchl P E 1994 Projector augmented-wave method *Phys. Rev. B* **50** 17953–79
- [25] Kresse G and Joubert D 1999 From ultrasoft pseudopotentials to the projector augmented-wave method *Phys. Rev. B* **59** 1758–75
- [26] Perdew J P, Burke K and Ernzerhof M 1996 Generalized gradient approximation made simple *Phys. Rev. Lett.* **77** 3865–8
- [27] Monkhorst H J and Pack J D 1976 Special points for brillouin-zone integrations *Phys. Rev. B* **13** 5188–92
- [28] Resende A, Jones R, Öberg S and Briddon P R 1999 Calculations of electrical levels of deep centers: application to Au-H and Ag-H defects in silicon *Phys. Rev. Lett.* **82** 2111–4
- [29] Istratov A A, Hieslmair H, Flink C, Heiser T and Weber E R 1997 Interstitial copper-related center in n-type silicon *Appl. Phys. Lett.* **71** 2349
- [30] Morin F J and Maita J P 1954 Electrical properties of silicon containing arsenic and boron *Phys. Rev.* **96** 28–35
- [31] Freysoldt C, Neugebauer J and Van de Walle C G 2009 Fully *ab initio* finite-size corrections for charged-defect supercell calculations *Phys. Rev. Lett.* **102**
- [32] Kumagai Y and Oba F 2014 Electrostatics-based finite-size corrections for first-principles point defect calculations *Phys. Rev. B* **89**
- [33] Makov G and Payne M C 1995 Periodic boundary conditions in *ab initio* calculations *Phys. Rev. B* **51** 4014–22
- [34] Sheppard D, Xiao P, Chemelewski W, Johnson D D and Henkelman G 2012 A generalized solid-state nudged elastic band method *J. Chem. Phys.* **136** 074103
- [35] Backlund D J and Estreicher S K 2010 Ti, Fe, and Ni in Si and their interactions with the vacancy and the A center: a theoretical study *Phys. Rev. B* **81**
- [36] Zhao S, Assali L V C, Justo J F, Gilmer G H and Kimerling L C 2001 Iron-acceptor pairs in silicon: structure and formation processes *J. Appl. Phys.* **90** 2744
- [37] Belayachi A, Heiser T, Schunck J P and Kempf A 2004 Influence of light on interstitial copper in p-type silicon *Appl. Phys. A* **80** 201–4
- [38] Brotherton S D, Ayres J R, Gill A, van Kesteren H W and Greidanus F J A M 1987 Deep levels of copper in silicon *J. Appl. Phys.* **62** 1826
- [39] Harris R D, Newton J L and Watkins G D 1982 Negative-*U* properties for interstitial boron in silicon *Phys. Rev. Lett.* **48** 1271–4